

# Effect of Hall Currents, Thermal Radiation Convective Heat Transfer Flow of a Rotating Nano-Fluid Past a Vertical Plate with Oscillatory Wall Velocity

Dr P. Srinivasa Rao

Department of Physics, Jyothshmathi Institute of Technology of Sciences, Karim Nagar-Telangana, India

## Abstract

We investigate the effect of thermal radiation and oscillatory wall velocity on unsteady convective heat transfer flow of a nanofluid past a vertical plate in the presence of heat generating sources. Analytical closed form solutions are obtained for both the momentum and the energy equations using the regular perturbation method. Graphs are used to illustrate the significance of key parameters on the nanofluid velocity and temperature distributions.

**Keywords:** Thermal Radiation, Heat transfer, Nanofluid, Vertical Plate

## 1. INTRODUCTION

Nanofluids are solid-liquid composite materials consisting of solid nanoparticles or nanofibers, with sizes typically on the order of 1–100 nm, suspended in a liquid. Nanofluids are characterized by an enrichment of a base fluid like water, toluene, ethylene glycol or oil with nanoparticles in variety of types like Metals, Oxides, Carbides, Carbon, Nitrides, etc. Today nanofluid are sought to have wide range of applications in medical application, biomedical industry, detergency, power generation in nuclear reactors and more specifically in any heat removal involved industrial applications. The ongoing research ever since then has extended to utilization of nanofluids in microelectronics, fuel cells, pharmaceutical processes, hybrid-powered engines, engine cooling, vehicle thermal management, domestic refrigerator, chillers, heat exchanger, nuclear reactor coolant, grinding, machining, space technology, Defense and ships, and boiler flue gas temperature reduction [Agarwal et al. (2011)]. Indisputably, the nanofluids are more stable and have acceptable viscosity and better wetting, spreading, and dispersion properties on a solid surface [Akbarinia et al. (2011), Nguyen et al. (2007)]. Several reviews [Ghadimi et al. (2011), Mahabudul et al. (2012)] on nanofluids with respect to thermal and rheological properties have been reported.

Thus, nanofluids have an ample collection of potential applications in electronics, pharmaceutical processes, hybrid-powered engines, automotive and nuclear applications where enhanced heat transfer or resourceful heat dissipation is required. In view of these, [Kiblinki et al. (2002)] suggested four possible explanations for the anomalous increase in the thermal conductivity of nanofluids. These are nanoparticles clustering, Brownian motion of the particles, molecular level layering of the liquid/particles interface and ballistic heat transfer in the nanoparticles. Despite a vast amount of literature on the flow of nanofluid model proposed by [Buongiorno (2006)], we are referring to a few recent studies [Alsaedi et al. (2012), Hajipour and Dekhordi (2012), Rana and Bhargava (2012)] in this article. However, we are following the nanofluid model proposed by [Tiwari and Das (2007)], which is being used by many current researchers [Hamad and Ferdows (2012), Hamad and Pop (2011), Norifiah et al. (2012)] on various flow fields.

The study of MHD flow and heat transfer due to the effect of a magnetic field in a rotating frame of reference has attracted the interest of many investigators in view of its applications in many industrial, astrophysical (dealing with the sunspot development, the solar cycle and the structure of a rotating magnetic stars), technological and engineering applications (MHD generators, ion propulsion, MHD pumps, etc.) and many other practical applications, such as in biomechanical problems (e.g., blood, flow in the pulmonary alveolar sheet). Many authors have studied the flow and heat transfer in a rotating system with various geometrical situations [Hickman (1957), Hide (1960), Mazumder (2012)]. [Hamad (2011)] investigated the effect of a transverse magnetic field on free convection flow of a nanofluid past a vertical semi-infinite flat plate. Recently, [Satya Narayana et al. (2013)] studied the Hall current and radiation absorption effects on MHD micropolar fluid in a rotating system. Some other related works can also be found in recent papers [Kameswaran et al. (2012), Kesavaiah et al. (2011), Rushi kumar and Sivaraj (2013), Srinivas et al. (2012)].

Thermal radiation is important in some applications because of the manner in which radiant emission depends on temperature and nanoparticles volume fraction. The thermal radiation effect on mixed convection heat transfer in porous media has many important applications such as the sensible heat storage bed, the nuclear reactor cooling system, space technology, and underground nuclear waste disposal. To the best of the author's knowledge (from the literature), no studies have been communicated thus far with regard to the study of flow and heat transfer distinctiveness of a nanofluid past a vertical plate with thermal radiation in a rotating frame of reference. [Salem and Aziz (2008)] have analyzed the effect of Hall currents and chemical reaction on the unsteady flow, heat and mass transfer laminar of a viscous, electrically conducting fluid over a continuously stretching surface in the presence of heat generation/absorption. [Aziz (2010)] investigated the flow and heat transfer of a viscous fluid

flow over a unsteady stretching surface with Hall effects. [Sarojamma et al. (2015)] have investigated the influence of Hall currents on cross diffusive convection in a MHD boundary layer flow on stretching sheet in porous medium with non-uniform heat source. Also [Sarojamma et al. (2015)] have discussed the effect of Hall currents on the flow induces by a stretching surface.

Recently [Satyanarayana et al (2011)] have studied the effect of radiation on the convective heat transfer flow of a rotating nanofluid past a porous vertical plate with oscillatory velocity.

In this paper we investigate the effect of Hall currents, thermal radiation on unsteady convective heat transfer flow of a nanofluid past a vertical plate in the presence of heat generating sources. Analytical closed form solutions are obtained for both the momentum and the energy equations using the regular perturbation method. Graphs are used to illustrate the significance of key parameters on the nanofluid velocity and temperature distributions.

### Nomenclature

$B_0$ : constant applied magnetic field  
 $C_f$ : skin friction coefficient  
 $E$ : applied electric field  
 $F$ : heat radiation parameter  
 $g$ : acceleration due to gravity  
 $K$ : permeability parameter  
  
 $k$ : permeability of porous medium  
 $k$ : mean absorption coefficient  
 $M$ : dimensionless magnetic field parameter  
 $Nu$ : local Nusselt number  
 $Nur$ : reduced Nusselt number  
 $Pr$ : Prandtl number  
 $Q$ : dimensional heat source parameter  
 $Q_H$ : dimensional heat source  
 $q_r$ : radiative heat flux  
 $q_w$ : heat flux from the plate  
 $R$ : dimensional rotational parameter  
 $Re_x$ : local Reynolds number  
 $S$ : suction parameter  
 $T$ : local temperature of the nanofluid  
 $T_w$ : wall temperature of the fluid  
 $T_\infty$ : temperature of the ambient nanofluid  
 $U_0$ : characteristic velocity  
 $w_0$ : normal velocity  
 $(x, y, z)$ : Cartesian coordinates  
 $(u, v, w)$ : velocity components along  $x$  and  $y$  axes

### Greek Symbols

$\alpha$ : thermal diffusivity  
 $\alpha_f$ : thermal diffusivity of the fluid  
 $\alpha_{nf}$ : thermal diffusivity of the nanofluid  
 $\beta$ : thermal expansion coefficient  
 $\beta_f$ : coefficient of thermal expansion of the fluid  
 $\beta_s$ : coefficient of thermal expansion of the solid  
 $\rho_f$ : density of the fluid friction  
 $\rho_s$ : density of the solid friction  
 $\rho_{nf}$ : density of the nanofluid  
 $n$ : kinematic viscosity  
 $n_f$ : kinematic viscosity of the fluid  
 $\mu$ : dynamic viscosity  
 $\mu_{nf}$ : viscosity of the nanofluid  
 $\sigma$ : electrical conductivity of the fluid  
 $\sigma^*$ : Stefan–Boltzmann constant parameter  
 $(\rho C)_{nf}$ : heat capacitance of the nanofluid  
 $\varepsilon$ : small constant quantity  
 $\chi$ : complex function  
 $\theta$ : non-dimensional temperature

### Subscripts

$f$ : fluid,  $s$ : solid  
 $nf$ : nanofluid  
 $w$ : condition at the wall  
 $\infty$ : condition at free stream

## 2. FORMULATION OF THE PROBLEM:

We consider an unsteady, three dimensional flow of a nanofluid consisting of a base fluid and small nanoparticles over a semi-infinite vertical porous plate with thermal radiation. A uniform magnetic field of strength  $H_0$  is applied normal to the plate. It is assumed that there is no applied voltage which implies the absence of an electric field. The flow is assumed to be in the  $x$ -direction which is taken along the plane in an upward direction and  $z$ -axis is normal to the plate. Also it is assumed that the whole system is rotating with a constant angular velocity vector  $\bar{\Omega}$  about the  $z$ -axis. The fluid is assumed to be gray, absorbing emitting but not scattering medium. The radiation heat flux in the  $x$ -direction is considered negligible in comparison with that in the  $z$ -direction. Due to a semi-infinite plate surface assumption, the flow variables are functions of  $z$  and  $t$  only. Figure. 1 shows that the problem under consideration and the co-ordinate system.

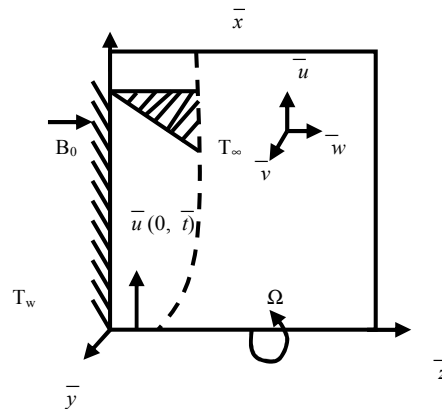


Figure 1 . Schematic diagram of the problem

In the present problem, the following assumptions have been made:

1. The plate has an oscillatory movement on time  $t$  and frequency  $n$  with velocity  $u(0,t)$ , which is given by  $\bar{u}(0,t) = U_0(1 + \varepsilon \text{Cos}(\bar{n}, \bar{t}))$
2. Initially  $\bar{t} < 0$  the fluids as well as the plate are at rest but for  $t \geq 0$  the whole system is allowed to rotate with a constant velocity  $\Omega$  about the  $z$ -axis.
3. It is assumed that there is no applied voltage which implies that an electric field is absent.
4. In a physically realistic situation, we cannot ensure perfect insulation in any experimental set-up. There will always be some fluctuations in the temperature. The plate temperature is assumed to vary harmonically with time. It varies from  $T_w^* + \varepsilon(T_w^* - T_\infty^*)$  as  $t$  varies from  $0$  to  $2\pi/\omega$ . Since  $\varepsilon$  is small, the plate temperature varies only slightly from the mean value  $T_w^*$ . The ambient temperature has the constant value  $T_\infty$ .
5. The conservation equation of current density  $\nabla \cdot \vec{J} = 0$  gives  $J_z = \text{constant}$ .  
 Under the above mentioned assumptions, the equation of momentum and thermal energy respectively, can be written in dimensional form as :

$$\frac{\partial w}{\partial z} = 0 \quad (2.1)$$

$$\frac{\partial u}{\partial t} + w \frac{\partial u}{\partial z} - 2\Omega v = \frac{1}{\rho_{nf}} \left( \mu_{nf} \frac{\partial^2 u}{\partial z^2} + (\rho \beta_{nf}) g(T - T_\infty) - \left(\frac{v_f}{k}\right)u + \frac{(\sigma \mu_e^2 H_o^2)}{1+m^2} (mv - u) \right) \quad (2.2)$$

$$\frac{\partial v}{\partial t} + w \frac{\partial v}{\partial z} + 2\Omega u = \frac{1}{\rho_{nf}} \left( \mu_{nf} \frac{\partial^2 v}{\partial z^2} - \left(\frac{v_f}{k}\right)v - \frac{(\sigma \mu_e^2 H_o^2)}{1+m^2} (mu + v) \right) \quad (2.3)$$

$$\frac{\partial T}{\partial t} + w \frac{\partial T}{\partial z} = k_{nf} \frac{\partial^2 T}{\partial z^2} - \frac{1}{(\rho C_p)_{nf}} \frac{\partial(q_r)}{\partial z} - \frac{Q_H}{(\rho C_p)_{nf}} (T - T_\infty) \quad (2.4)$$

The boundary conditions are (see ref.(42&43)):

$$u(z,t) = 0, v(z,t) = 0, T = T_w \quad \text{for } z \leq 0, \text{ and any } z$$

$$u(0,t) = U_0 \left( 1 + \frac{\varepsilon}{2} (e^{i\omega t} + e^{-i\omega t}) \right), v(0,t) = 0, T(0,t) = T_w \quad (2.5)$$

$$u(\infty,t) \rightarrow 0, v(\infty,t) \rightarrow 0, T(\infty,t) \rightarrow T_\infty, \quad \text{for } t \geq 0$$

The properties of the nanofluids are defined as follows (see ref.(44-46)):

$$\left. \begin{aligned} \mu_{nf} &= \mu_f / (1 - \phi)^{2.5} & \alpha_{nf} &= \frac{k_{nf}}{(\rho C_p)_{nf}} & \rho_{nf} &= (1 - \phi)\rho_f + \phi\rho_s \\ (\rho C_p)_{nf} &= (1 - \phi)(\rho C_p)_f + \phi(\rho C_p)_s & (\rho\beta)_{nf} &= (1 - \phi)(\rho\beta)_f + \phi(\rho\beta)_s \end{aligned} \right\} \quad (2.6)$$

$$k_{nf} = \frac{k_f(k_s + 2k_f - 2\phi(k_f - k_s))}{(k_s + 2k_f + 2\phi(k_f - k_s))}$$

We consider the solution of equation(2.1) as:

$$w = -w_0 \quad (2.7)$$

The radiation heat term(Brewster(47))by using The Rosseland approximation is given by

$$q_r = -\frac{4\sigma^* \partial T'^4}{3\beta_R \partial z} \quad (2.8)$$

$$T'^4 \cong 4TT_\infty^3 - 3T_\infty^4 \quad (2.9)$$

$$\frac{\partial q_R}{\partial z} = -\frac{16\sigma^* T_\infty^3}{3\beta_R} \frac{\partial^2 T}{\partial z^2} \quad (2.10)$$

We introduce the following dimensionless variables:

$$\left. \begin{aligned} z' &= \left(\frac{U_0}{v_f}\right)z, \quad t' = \left(\frac{U_0^2}{v_f}\right)t, \quad n' = \left(\frac{v_f}{U_0^2}\right)n, \quad u' = \frac{u}{U_0}, \quad v' = \frac{v}{U_0}, \quad \theta = \frac{T - T_\infty}{T_w - T_\infty}, \quad m = \omega_e \tau_e \\ S &= \frac{w_0}{U_0}, \quad M = \frac{\sigma \mu_e^2 H_0^2 v_f}{\rho_f U_0^2}, \quad R = \frac{2\Omega v_f}{U_0^2}, \quad Q = \frac{Q_H v_f^2}{k_f U_0^2}, \quad F = \frac{4\sigma^* T_\infty^3}{\beta_R k_f}, \quad D^{-1} = \frac{v_f^2}{\rho_f k_f U_0^2} \end{aligned} \right\} \quad (2.11)$$

Equations(2.2)-(2.4) in the non-dimensional form are

$$\frac{\partial u}{\partial t} - S \frac{\partial u}{\partial z} - Rv = \frac{1}{A_1 A_3} \frac{\partial^2 u}{\partial z^2} + \frac{A_4}{A_3} G\theta - \frac{\left(\frac{mM^2}{1+m^2} + D^{-1}\right)}{A_3} u + \frac{\left(\frac{mM^2}{1+m^2}\right)}{A_3} v \quad (2.12)$$

$$\frac{\partial v}{\partial t} - S \frac{\partial v}{\partial z} + Ru = \frac{1}{A_1 A_3} \frac{\partial^2 v}{\partial z^2} - \frac{\left(\frac{mM^2}{1+m^2} + D^{-1}\right)}{A_3} v - \frac{\left(\frac{mM^2}{1+m^2}\right)}{A_3} u \quad (2.13)$$

$$\frac{\partial \theta}{\partial t} - S \frac{\partial \theta}{\partial z} = \frac{1}{P_r} \left( \frac{A_2}{A_5} \frac{\partial^2 \theta}{\partial z^2} - \frac{1}{A_5} Q\theta \right) \quad (2.14)$$

Where

$$A_1 = (1 - \phi)^{2.5} \quad A_2 = \frac{k_{nf}}{k_f} + \frac{4F}{3}, \quad A_3 = 1 - \phi + \phi \left( \frac{\rho_s}{\rho_f} \right)$$

$$A_4 = 1 - \phi + \phi \left( \frac{(\rho\beta)_s}{(\rho\beta)_f} \right), \quad A_5 = 1 - \phi + \phi \left( \frac{(\rho C_p)_s}{(\rho C_p)_f} \right)$$

The boundary conditions (2.5) reduce to

$u(z,t) = 0, \quad v(z,t) = 0, \quad \theta(z,t) = 0 \quad \text{for } t \leq 0 \text{ and any } z$

$$u(0,t) = 1 + \frac{\mathcal{E}}{2}(e^{i\omega t} + e^{-i\omega t}), \quad v(0,t) = 0, \quad \theta(0,t) = 1 \quad (2.15)$$

$u(\infty,t) \rightarrow 0, \quad v(\infty,t) \rightarrow 0, \quad \theta(\infty,t) \rightarrow 0 \quad \text{for } t \geq 0$

Using (2.12) the velocity characteristic  $U_0$  is defined as:

In view of the fluid velocity in the component form:

$$V(z,t)u(z,t) + iv(z,t)$$

The equations (2.12) and (2.13) reduce to

$$\frac{\partial V}{\partial t} - S \frac{\partial V}{\partial z} + iRV = \frac{1}{A_1 A_3} \frac{\partial^2 v}{\partial z^2} + \frac{A_4}{A_3} \theta - \frac{(M^2(1-im)) + D^{-1}}{1+m^2} \frac{1}{A_2} V \quad (2.16)$$

The boundary conditions(2.15) reduce to

$$V(z,t) = 0 \quad \theta(z,t) = 0 \quad \text{for } t \leq 0 \text{ any } z$$

$$V(0,t) = 1 + \frac{\mathcal{E}}{2}(e^{i\omega t} + e^{-i\omega t}) \quad \theta(0,t) = 1 \quad (2.17)$$

$$V(z,t) \rightarrow 0, \quad \theta(z,t) \rightarrow 0 \quad \text{for } t \geq 0$$

### 3. METHOD SOLUTION:

Equations (2.14) and (2.16) are coupled, non-linear partial differential equations and these can not be solved in closed form. However, these equations can be reduced to a set of ordinary differential equations, which can be solved analytically. This can be done representing the velocity and temperature of the fluid in the neighborhood of the plate.

$$V(z,t) = V_0(Z,T) + \frac{\mathcal{E}}{2}(e^{i\omega t} V_1(z) + e^{-i\omega t} V_2(z)) \quad (2.18)$$

$$\theta(z,t) = \theta_0(z,t) + \frac{\mathcal{E}}{2}(e^{i\omega t} \theta_1(z) + e^{-i\omega t} \theta_2(z)) \quad (2.19)$$

Substituting the above Equations (2.18)&(2.19)in equations(2.14) and (2.16) and equating the harmonic and non-harmonic terms and neglecting the higher order terms of  $O(\mathcal{E}^2)$  .we obtain the following set of equations:

#### a) ZEROth ORDER EQUATIONS:

$$\frac{d^2 V_0}{dz^2} + A_3 S \frac{dV_0}{dz} - A_1(iRA_3 + M_1^2)V_0 + A_1 A_4 \theta_0 = 0 \quad (2.20)$$

$$A_2 \frac{d^2 \theta_0}{dz^2} + A_5 S \text{Pr} \frac{d\theta_0}{dz} - Q\theta_0 = 0 \quad (2.21)$$

First order equations:

$$\frac{d^2 V_1}{dz^2} + A_3 S \frac{dV_1}{dz} - A_1(i(R + \omega)A_3 + M_1^2)V_1 + A_1 A_4 \theta_1 = 0 \quad (2.22)$$

$$A_2 \frac{d^2 \theta_1}{dz^2} + A_5 S \text{Pr} \frac{d\theta_1}{dz} - (i\omega \text{Pr} A_5 + Q)\theta_1 = 0 \quad (2.23)$$

#### b) SECONd OREDER EQUATIONS:

$$\frac{d^2 V_2}{dz^2} + A_3 S \frac{dV_2}{dz} - A_1(i(R - \omega)A_3 + M_1^2)V_2 + A_1 A_4 \theta_2 = 0 \quad (2.24)$$

$$A_2 \frac{d^2 \theta_2}{dz^2} + A_5 S \text{Pr} \frac{d\theta_2}{dz} - (i\omega \text{Pr} A_5 - Q)\theta_{2+} = 0 \quad (2.25)$$

The corresponding transformed boundary conditions are

$$\begin{aligned} V_0 = 1, \theta_0 = 1, V_1 = 1, \theta_1 = 0, V_2 = 1, \theta_2 = 0 \quad \text{at } z = 0 \\ V_0 \rightarrow 0, \theta_0 \rightarrow 0, V_1 \rightarrow 0, \theta_1 \rightarrow 0, V_2 \rightarrow 0, \theta_2 \rightarrow 0 \quad \text{at } z \rightarrow 0 \end{aligned} \quad (2.26)$$

Solving equations(2.21)-(2.25) with the boundary conditions (2.26) we obtain the expressions for the velocity and temperature as:

$$V(z) = V_o(z) + \frac{\varepsilon}{2} (V_1(z) \exp(i\omega t) + V_2(z) \exp(-i\omega t))$$

$$\theta(z) = \theta_o(z) + \frac{\varepsilon}{2} (\theta_1(z) \exp(i\omega t) + \theta_2(z) \exp(-i\omega t))$$

Where

$$V_0(z) = B_1 \exp(-m_1 z) + (1 - B_1) \exp(-m_2 z)$$

$$V_1(z) = B_2 \exp(-m_3 z) + (1 - B_2) \exp(-m_4 z)$$

$$V_2(z) = B_3 \exp(-m_5 z) + (1 - B_3) \exp(-m_6 z)$$

$$\theta_0(z) = \exp(-m_1 z)$$

The physical quantities of interest are skin friction and Nusselt number which are, respectively, defined as:

$$C_f = \frac{\tau_w}{\rho_f U_o^2}$$

$$Nu = \frac{xq_w}{k_f (T_w - T_\infty)}$$

Where  $\tau_w$  and  $q_w$  are the wall shear and the wall heat flux from the plate respectively, which are given by

$$\tau_w = \mu_{nf} \left( \frac{\partial u}{\partial z} \right)_{z=0} \quad \text{and} \quad q_w = -k_{nf} \left( \frac{\partial T}{\partial z} \right)_{z=0}$$

In view of Equation (2.11) we obtain

$$\begin{aligned} C_f = \frac{1}{(1-\phi)^{2.5}} V'(0) = -\frac{1}{A_1} ((B_1 - 1)m_2 - B_1 m_1 + \frac{\varepsilon}{2} ((B_2 - 1)m_4 - B_2 m_3) \exp(i\omega t) + \\ + ((B_3 - 1)m_6 - B_3 m_5) \exp(-i\omega t)) \end{aligned}$$

$$Nu = -\frac{k_{nf}}{k_f} \theta'(0) = \frac{k_{nf}}{k_f} (m_1)$$

Where

$$M_1^2 = \frac{M^2(1-im)}{1+m^2} + D^{-1} \quad m_1 = \frac{A_5 S \text{Pr} + \sqrt{(A_5 S \text{Pr})^2 + 4A_2 Q}}{2A_2}, \quad \beta_1^2 = iRA_3 + M_1^2$$

$$m_2 = \frac{A_3 S + \sqrt{(A_3 S)^2 + 4\beta_1^2}}{2}, \quad \beta_2^2 = i\omega \text{Pr} A_5 + Q_1$$

$$m_4 = \frac{A_3 S + \sqrt{(A_3 S)^2 + 4\beta_3^2}}{2}, \quad \beta_4^2 = i\omega \text{Pr} A_5 - Q_1$$

$$m_6 = \frac{A_3 S + \sqrt{(A_3 S)^2 + 4\beta_5^2}}{2}, \quad B_1 = -\frac{A_2 A_4}{m_1^2 - m_1 A_3 S - \beta_1^2}$$

$$B_2 = -\frac{A_1 A_4}{m_3^2 - m_{31} A_3 S - \beta_3^2}, \quad B_3 = -\frac{A_1 A_4}{m_5^2 - m_5 A_3 S - \beta_5^2}$$

#### 4. DISCUSSION OF THE NUMERICAL RESULTS:

A mathematical assessment for the analytical solution of this problem is performed, and the outcomes are illustrated graphically in Figures 1- 8. They explain the fascinating features of important parameters on the nanofluid velocity, temperature, skin friction and Nusselt number distributions in a rotating system for three different types of water based nanofluids. As in [Oztop and Abu-Nada (2008)], we take the values of the nanofluid volume fraction  $\phi$  in the range of  $0 \leq \phi \leq 0.08$ . We considered for the convective flow in a lid driven cavity, the value of the nanofluid volume fraction in the range  $0 \leq \phi \leq 0.08$ . If the concentration exceeds the maximum level of 0.08, sedimentation could take place. We have chosen here  $n = 10$ ,  $nt = \pi/2$ ,  $\varepsilon = 0.02$ ,  $Pr = 6.2$  while  $M$ ,  $R$ ,  $S$ ,  $\phi$ ,  $Q$ ,  $F$  are varied over a range, which are listed in the Figure legends.

Fig.2a represents the effect of magnetic field on the nanofluid velocity profile. It is found that the nanofluid velocity field reduces with increase of magnetic field parameter  $M$  along the surface. These effects are much significant near the surface of the plate. This shows that the fluid velocity is reduced by increasing the magnetic field and confirms the fact that the application of the magnetic field to an electrically conducting fluid produces a drag like force which causes a retardation in the fluid velocity. From Fig.2b, it is interesting to note that the effect of magnetic parameter on the secondary velocity is to reduce the magnitude of  $v$ . It is seen that the velocity rapidly increases attaining maximum at  $y=3$  and then reduces to attain the prescribed value zero far away from the boundary. We also find that the nano fluid velocity in the case of  $CuO_2$  – water nanofluid is relatively lesser than that of  $Al_2O_3$ -water nanofluid in the case of primary velocity while in the case of secondary velocity, its value in  $CuO$ -water is greater than that of  $Al_2O_3$ -water. This phenomenon has good agreement with the physical realities.

Fig.3a represents the effect of inverse Darcy parameter  $D^{-1}$  on the nanofluid velocity profile. It is observed from the Figure that the velocity distribution decreases with increasing the inverse Darcy parameter  $D^{-1}$ . This is due to the fact that increase in the obstruction of the fluid motion with increase in the inverse Darcy parameter (since permeability of the porous medium appears in the denominator of the inverse Darcy parameter), thereby increase in inverse Darcy parameter indicates decrease in the permeability of the porous medium so the fluid velocity decrease. The effect of porous permeability parameter on the secondary velocity is shown in Fig.3b. It is found that the magnitude of  $v$  reduces with increase in  $D^{-1}$ . The peak value of the secondary velocity is attained at  $y=2$ . We also find that the nano-fluid velocity in the case of  $CuO_2$  – water nanofluid is relatively greater than that of  $Al_2O_3$ -water nanofluid. This phenomenon has good agreement with the physical realities.

Fig.4a represents the nanofluid velocity distribution with Hall parameter ( $m$ ). It is found that the velocity enhances with increase in the Hall parameter. This is due to the fact the thickness of the boundary layer increases with increase in Hall parameter. From Fig.4b we find that the secondary velocity enhances in magnitude with increase in the Hall parameter ( $m$ ) in both types of nanofluids. We observe that the nano fluid velocity in the case of  $CuO$ -water nanofluid is relatively lesser than that of  $Al_2O_3$ -water nanofluid. While in the case of secondary velocity, we notice that its values on  $CuO$ -water nanofluid is greater than that of  $Al_2O_3$ -water nanofluid. This phenomenon has good agreement with the physical realities.

Fig.5a represents the nanofluid velocity profiles for different values of rotational parameter  $R$ . This result displays that the nanofluid velocity reduces with an increase in  $R$ , as noted in reference [Hamad et al. (2011)]. Fig.4b depicts the variation of the secondary velocity with rotation parameter ( $R$ ). It is observed from the profiles that the magnitude of  $v$  enhances with increase in  $R$ . Further, we find that the  $Al_2O_3$ -water nanofluid exhibits lower velocity than the flow as compared to the  $CuO$ -water nanofluid.

Fig.6a shows that the nanofluid velocity with suction parameter  $S$  in the case of  $CuO$  and  $Al_2O_3$  nanoparticles. It can be seen from the profiles that the nanofluid primary velocity reduces for higher  $S$  which indicates that the suction stabilizes the boundary layer growth. The free convection effect is also apparent in this Figure. The effect of  $S$  on the nanofluid velocity is the reverse in the case of [Hamad et al. (2013)]. This is due to the dominate role of the radiation in the fluid field. Fig.6b depicts  $v$  with Suction parameter  $S$ . It is noticed that  $|v|$  reduces with increase in  $S$ . These results are clearly supported from the physical point of view. We also notice that  $Al_2O_3$ -water nanofluid has lesser velocity profiles than the  $CuO$ -water nanofluid. The variation of temperature with suction parameter  $S$  is exhibited in Fig.6c. It can be seen from the profiles that the temperature reduces with increase in  $S$  in both types of nanofluids. We also observe that the temperature in  $CuO_2$ -water nanofluid is greater than that of  $Al_2O_3$ -water nanofluid.

Figs.7a&&7b depict the behavior of the primary and secondary velocities with heat source parameter  $Q$ . It is found that the both components of velocities exhibit a decreasing tendency with increase in the strength of the

heat source. This is due to the fact that when heat is absorbed, the buoyancy forces decreases which reduces the flow rate and there by gives rise to a depreciation in the velocity component profiles. Fig.7c represents the temperature (T) with Heat source parameter Q. It is observed from the profiles that an increase in Q reduces the temperature and hence the thickness of the thermal boundary layer reduces with increase in Q in both types of nanofluids. We also find that the values of temperature in CuO<sub>2</sub>-water nanofluid are relatively higher than that of Al<sub>2</sub>O<sub>3</sub>-water nanofluid.

The variation of primary and secondary velocities with Prandtl number Pr is exhibited in Figs.8a&8b. It is found that the primary and secondary velocity components show a depreciation with increasing the values of Prandtl number and hence the thickness of the boundary layer also reduces in both types of nanofluids. Fig.8c shows the variation of temperature with Pr. It is found that an increase in Pr<2 reduces the temperature in the thermal boundary layer and for higher values of Pr>3, we notice an enhancement in the temperature. Thus lesser the thermal diffusivity smaller the temperature and for further lowering of the thermal diffusivity larger the temperature in the boundary layer.

Figs.9a&9b display the effect of nanoparticle volume fraction  $\phi$  on the nanofluid velocity and secondary velocity respectively. It is found that as the nanoparticle volume fraction increases the nanofluid primary velocity experiences an enhancement while the secondary velocity component reduces in the boundary layer. These Figures illustrate this agreement with the physical behavior. When the volume of the nanoparticle increases, the thermal conductivity and the thermal boundary layer thickness increase. We also notice that the nanofluid velocity in the case of Al<sub>2</sub>O<sub>3</sub> – water nanofluid is relatively greater than that of Cu-water nanofluid in the case of primary velocity while in case of secondary velocity, its values in CuO-water nanofluid is greater than that of Al<sub>2</sub>O<sub>3</sub>-water. Fig.9c shows that T with  $\phi$ . It can be seen from the profiles that an increase in the nanoparticle volume fraction enhances the temperature in the boundary layer. This is due to the fact that the thickness of the thermal boundary layer increases with increase in  $\phi$ . Also we find that the temperature in Al<sub>2</sub>O<sub>3</sub>-water is relatively lesser than that of Cu-water fluid.

Figs.10a & 10b exhibit the nanofluid primary and secondary velocity components for various values of radiation parameter F. An increase in F leads to an enhancement in the primary and secondary velocity distributions across the boundary layer. The effect of thermal radiation is to enhance heat transfer because of the fact that thermal boundary layer thickness increases with an increase in the thermal radiation. Fig.10c represents T with radiation parameter F. It can observe that an increase in F results in an increase in T. This is attributed to the fact that an enhancement of the radiation parameter results in an increase of thickness of the thermal boundary layer. Thus it is pointed out that the radiation should be minimized to have the cooling process at a faster rate. We also find that secondary nanofluid velocity and temperature in the case of Al<sub>2</sub>O<sub>3</sub>-water nanofluid is comparatively less than that of Cu-water nanofluid while in the case of CuO-water, its values of velocity is greater than that of Al<sub>2</sub>O<sub>3</sub>-water nanofluid. This occurrence has a superior agreement with the physical relatives.

Table.3 displays the behavior of local skin friction components  $\tau_x$  and  $\tau_y$  and Nusselt number Nu at the plate  $y=0$ . It is found that an increase in the Hartmann number M and inverse Darcy parameter reduces  $\tau_x$  and  $\tau_y$  while an increase in the rotation parameter R reduces  $\tau_x$  and enhances  $\tau_y$  at  $y=0$ . The components of skin friction enhances with increase in Hall parameter (m). Also  $\tau_x$  and  $\tau_y$  enhances with increase in the suction parameter S and the radiation parameter F and enhances  $\tau_x$ , reduces  $\tau_y$  at  $y=0$  with increase in the strength of the heat generating source Q for Cu-water nanofluid. An increase in the nanoparticle volume fraction  $\phi$  enhances  $\tau_x$  and  $\tau_y$  for Cu-water nanofluid.

In the case of Al<sub>2</sub>O<sub>3</sub>-water nanofluid an increase in M,  $D^{-1}$ , S, R, F and  $\phi$  enhances the skin friction component  $\tau_x$  and it reduces with increase in Hall parameter (m) or heat source parameter  $Q_1$ . An increase in the nanoparticle concentration  $\phi$  leads to an enhancement in  $\tau_x$ . Its variation with respect to Prandtl number Pr shows that lesser the thermal diffusivity (Pr<3) smaller  $\tau_x$  and for further lowering of the thermal diffusivity (Pr>6.2) we find an enhancement in it. An increase in M,  $D^{-1}$ ,  $Q_1$  and Pr results in a depreciation in  $\tau_y$ . an increase in the Hall parameter  $m \leq 1$  leads to a depreciation and for higher  $m \geq 1.5$ , we find an enhancement in  $\tau_y$ . Also it enhances with increase in R, S and F. An increase in the nanoparticle concentration  $\phi$  increases the skin friction component ( $\tau_y$ ) at the wall  $y=0$ . We find that the magnitude of the skin friction components in Al<sub>2</sub>O<sub>3</sub>-water nanofluid have lesser values than that of the skin friction components in the case of CuO-water nanofluid.

The local Nusselt number (Nu) at  $y=0$  is found to enhance with increase in S or Q or Pr and reduces with increase in radiation parameter F for both Cu-water and Al<sub>2</sub>O<sub>3</sub> – water nanofluids. An increase in  $\phi$  reduces |Nu| at  $y=0$  for Cu-water nanofluid and enhances in the case of Al<sub>2</sub>O<sub>3</sub>-water nanofluids. We also observe that the values of |Nu| in CuO-water nanofluid are higher than that of Al<sub>2</sub>O<sub>3</sub>-water nanofluid .



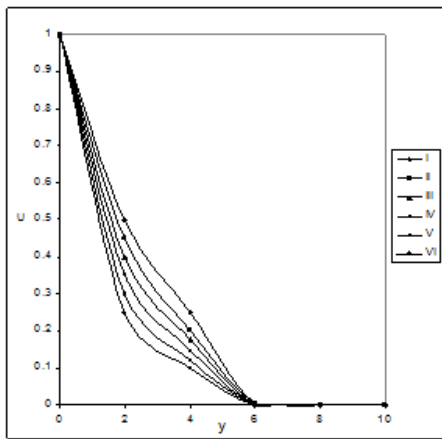


Fig. 2a Variation of u with M  
 I II III IV V VI  
 Cu-water Al<sub>2</sub>O<sub>3</sub>-water  
 M 0.2 1 1.5 0.2 1 1.5

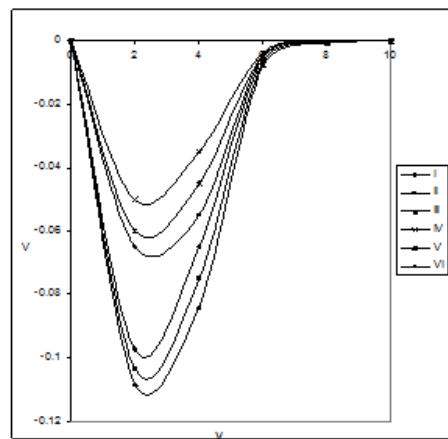


Fig.2b Variation of v with M  
 I II III IV V VI  
 Cu-water Al<sub>2</sub>O<sub>3</sub>-water  
 M 0.2 1 1.5 0.2 1 1.5

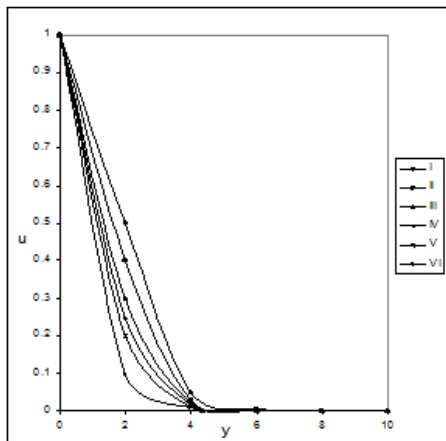


Fig.3a Variation of u with D<sup>-1</sup>  
 I II III IV V VI  
 Cu-water Al<sub>2</sub>O<sub>3</sub>-water  
 D<sup>-1</sup> 10<sup>2</sup> 2x10<sup>2</sup> 3x10<sup>2</sup> 10<sup>2</sup> 2x10<sup>2</sup> 3x10<sup>2</sup>

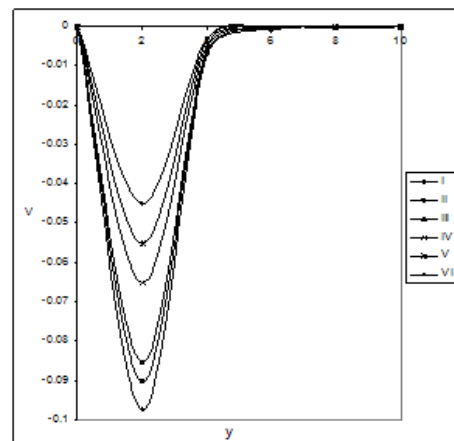


Fig.3b Variation of v with D<sup>-1</sup>  
 I II III IV V VI  
 Cu-water Al<sub>2</sub>O<sub>3</sub>-water  
 D<sup>-1</sup> 10<sup>2</sup> 2x10<sup>2</sup> 3x10<sup>2</sup> 10<sup>2</sup> 2x10<sup>2</sup> 3x10<sup>2</sup>

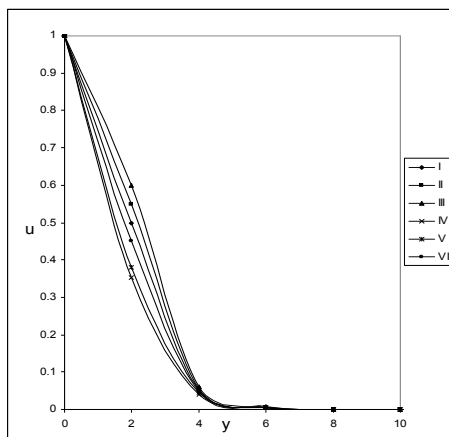


Fig.4a Variation of u with m  
 I II III IV V VI  
 Cu-water Al<sub>2</sub>O<sub>3</sub>-water  
 m 0.5 1 1.5 0.5 1 1.5

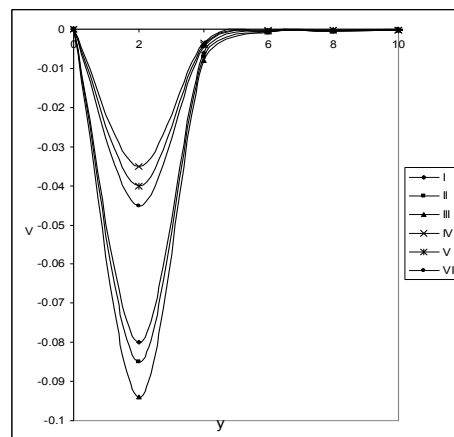


Fig.4b Variation of v with m  
 I II III IV V VI  
 Cu-water Al<sub>2</sub>O<sub>3</sub>-water  
 m 0.5 1 1.5 0.5 1 1.5

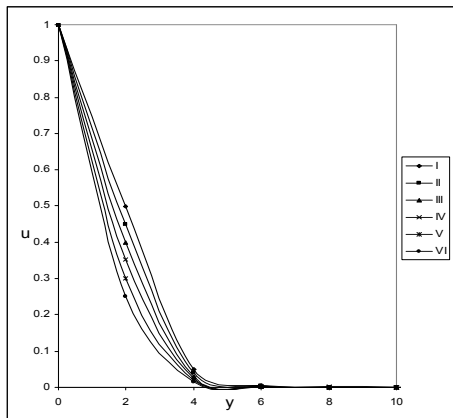


Fig.5a Variation of  $u$  with  $R$   
 I II III IV V VI  
 Cu-water  $Al_2O_3$ -water  
 $R$  0.02 0.04 0.06 0.02 0.04 0.06

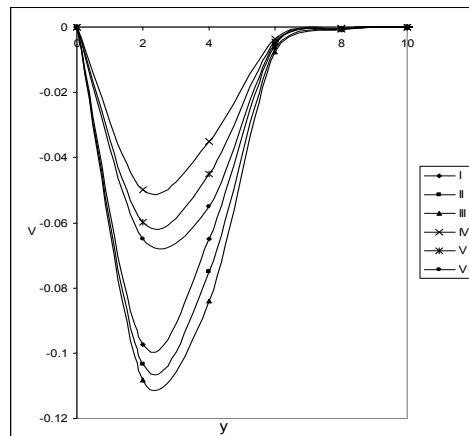


Fig.5b Variation of  $v$  with  $R$   
 I II III IV V VI  
 Cu-water  $Al_2O_3$ -water  
 $R$  0.02 0.04 0.06 0.02 0.04 0.06

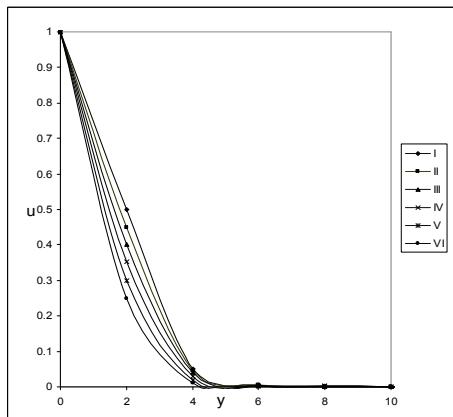


Fig. 6a Variation of  $u$  with  $s$   
 I II III IV V VI  
 Cu-water  $Al_2O_3$ -water  
 $s$  0.1 0.4 0.1 0.2 0.4

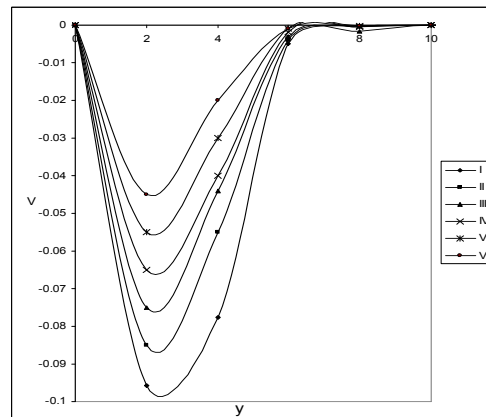


Fig. 6b Variation of  $v$  with  $s$   
 I II III IV V VI  
 Cu-water  $Al_2O_3$ -water  
 $s$  0.1 0.4 0.1 0.2 0.4

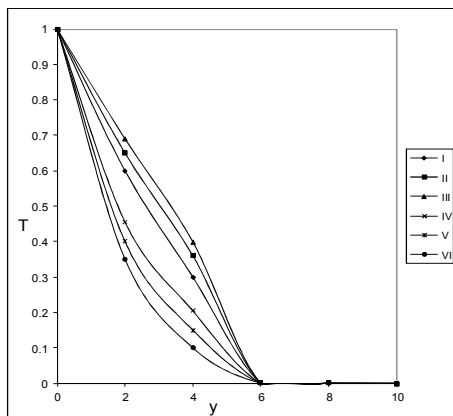


Fig. 6c Variation of  $T$  with  $s$   
 I II III IV V VI  
 Cu-water  $Al_2O_3$ -water  
 $s$  0.1 0.4 0.1 0.2 0.4

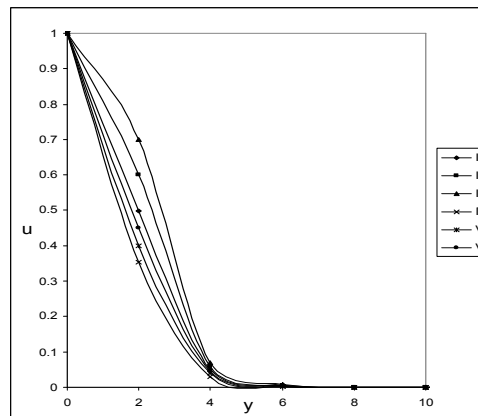


Fig.7a Variation of  $u$  with  $Q$   
 I II III IV V VI  
 Cu-water  $Al_2O_3$ -water  
 $Q$  2 4 6 2 4 6

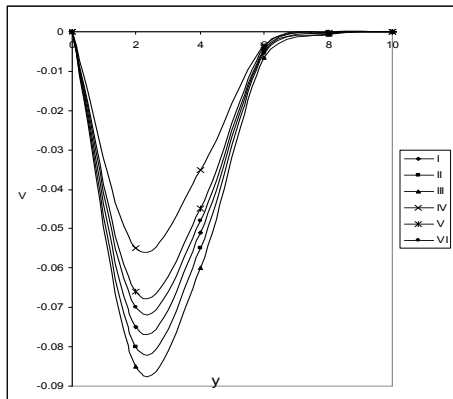


Fig.7b Variation of  $v$  with  $Q$   
 I II III IV V VI  
 Cu-water Al<sub>2</sub>O<sub>3</sub>-water  
 $Q$  2 4 6 2 4 6

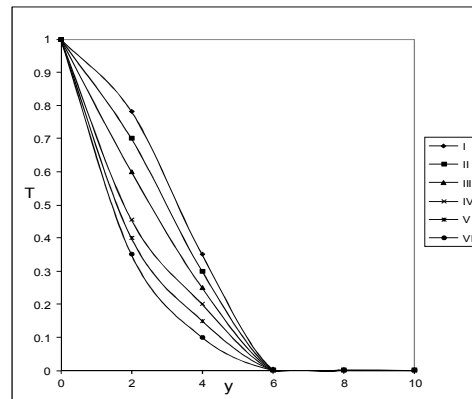


Fig.7c Variation of  $T$  with  $Q$   
 I II III IV V VI  
 Cu-water Al<sub>2</sub>O<sub>3</sub>-water  
 $Q$  2 4 6 2 4 6

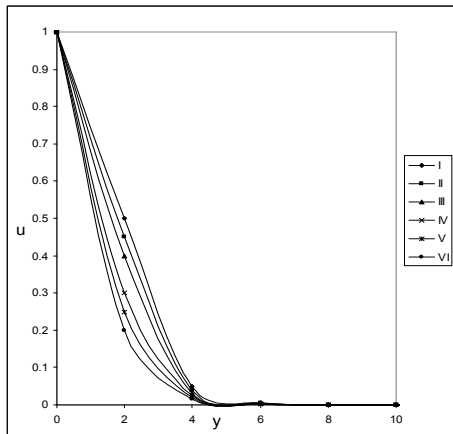


Fig.8a Variation of  $u$  with  $Pr$   
 I II III IV V VI  
 Cu-water Al<sub>2</sub>O<sub>3</sub>-water  
 $Pr$  0.71 3 6.2 0.71 3 6.2

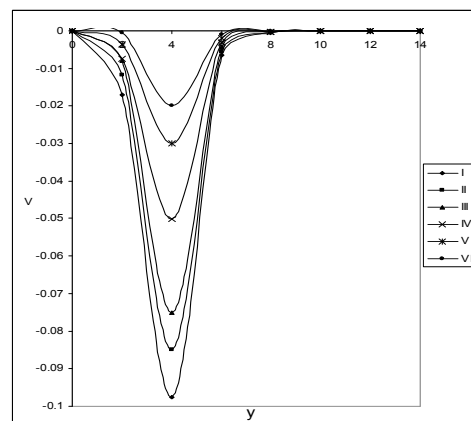


Fig.8b Variation of  $v$  with  $Pr$   
 I II III IV V VI  
 Cu-water Al<sub>2</sub>O<sub>3</sub>-water  
 $Pr$  0.71 3 6.2 0.71 3 6.2

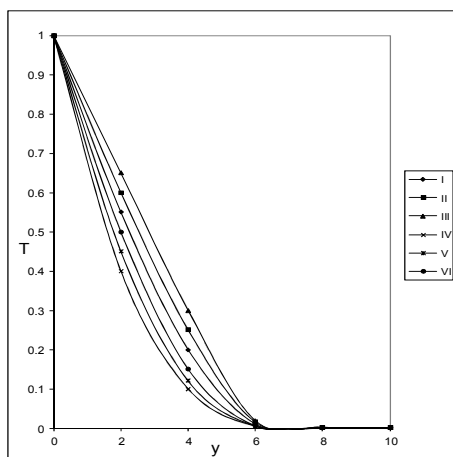


Fig.8c Variation of  $T$  with  $Pr$   
 I II III IV V VI  
 Cu-water Al<sub>2</sub>O<sub>3</sub>-water  
 $Pr$  0.71 3 6.2 0.71 3 6.2

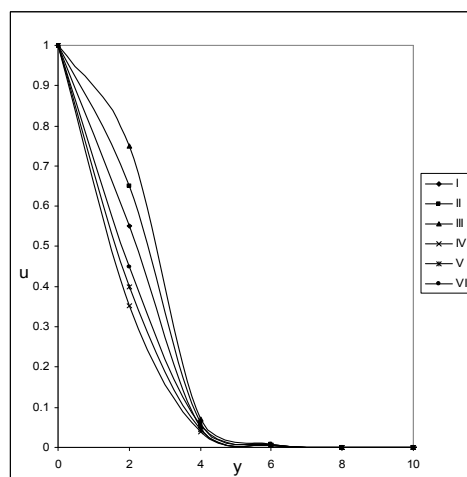


Fig.9a Variation of  $u$  with  $\phi$   
 I II III IV V VI  
 Cu-water Al<sub>2</sub>O<sub>3</sub>-water  
 $\phi$  0.1 0.3 0.5 0.1 0.3 0.5

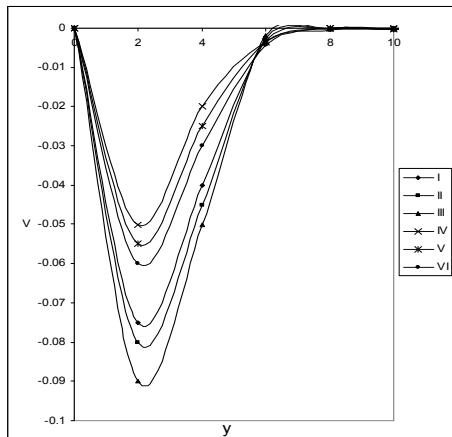


Fig.9b Variation of  $v$  with  $\phi$   
 I II III IV V VI Cu-water  
 Al<sub>2</sub>O<sub>3</sub>-water  
 $\phi$  0.1 0.3 0.5 0.1 0.3 0.5

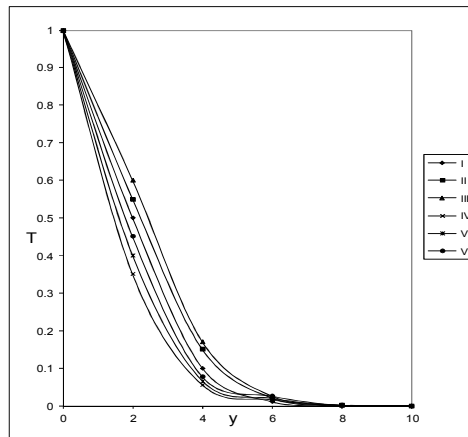


Fig.9c Variation of  $T$  with  $\phi$   
 I II III IV V VI Cu-water  
 Al<sub>2</sub>O<sub>3</sub>-water  
 $\phi$  0.1 0.3 0.5 0.1 0.3 0.5

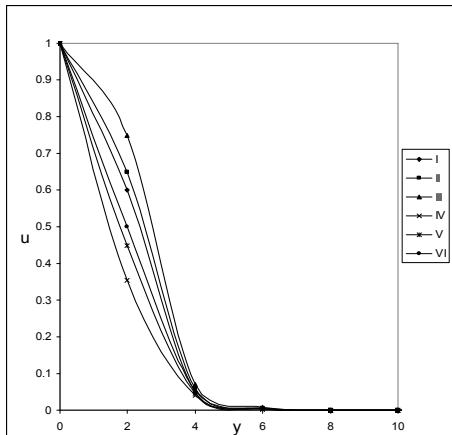


Fig.10a Variation of  $u$  with  $F$   
 I II III IV V VI Cu-water  
 Al<sub>2</sub>O<sub>3</sub>-water  
 $F$  0.5 1.5 2.5 0.5 1.5 2.5

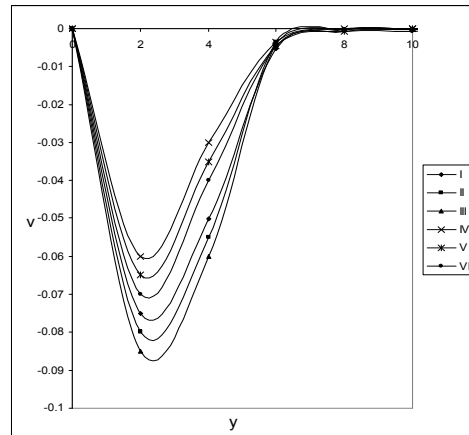


Fig.10b Variation of  $v$  with  $F$   
 I II III IV V VI Cu-water  
 Al<sub>2</sub>O<sub>3</sub>-water  
 $F$  0.5 1.5 2.5 0.5 1.5 2.5

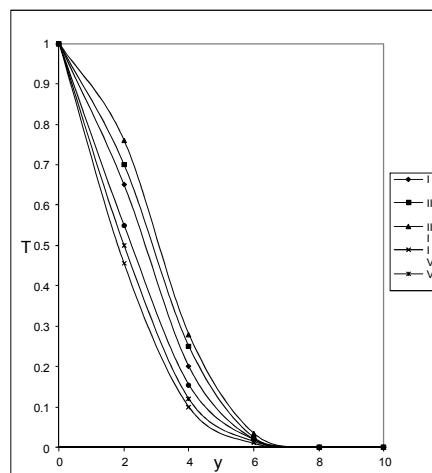


Fig.10c Variation of  $T$  with  $F$   
 I II III IV V VI Cu-water  
 Al<sub>2</sub>O<sub>3</sub>-water  
 $F$  0.5 1.5 2.5 0.5 1.5 2.5

Table 1 : Thermo-physical properties of water and nanoparticles

Physical properties	Water	Cu	Al <sub>2</sub> O <sub>3</sub>
C <sub>p</sub> (J/kg K)	4179	385	765
ρ (kg/m <sup>3</sup> )	997.1	8933	3970
K (W/m K)	0.613	400	40
β X 10 <sup>-5</sup> (1/K)	21	1.67	0.85

Table 2 : Comparison of skin friction and Nusselt number of the present case with those of Hamad et al. (2011), In the absence of Hall currents(m=0.0)

Pr	Skin Friction			Nusselt Number		
	ε=0.02, F=1.0, R=0.02, n=10.0, t=0.1, M=0.5, Q=10.0, φ=0.15, S=1.0, m=0.0			S=1.0, F=0.1, Q = 10.0, φ=0.15, m=0.0		
	Present	Satyanarayana et al [21]	Hamad et al [8]	Present	Satyanarayana et al [21]	Hamad et al [8]
0.5	2.3101	2.3159708	2.3202	5.9642	5.9674231	5.9674
1.0	2.2581	2.2567503	2.2586	6.0459	6.0461932	6.0461
1.5	2.1969	2.1972895	2.1967	6.1255	6.1259433	6.1259
2.0	2.1371	2.1376083	2.1345	6.2059	6.2066709	6.2066

Table 3

		CuO <sub>2</sub>			Al <sub>2</sub> O <sub>3</sub>		
		τ <sub>x</sub> (0)	τ <sub>y</sub> (0)	Nu(0)	τ <sub>x</sub> (0)	τ <sub>y</sub> (0)	Nu(0)
M	0.5	64.5393	-7.2536	-----	-17.8833	0.8853	-----
	1.5	64.2357	-7.0694		-17.8117	0.8862	
	2.5	63.8438	-6.8349		-17.7507	0.8881	
S	0.1	64.5393	-7.2536	-81.5514	-17.8833	0.8853	25.7847
	0.5	67.1482	-7.5606	-83.7865	-18.1623	0.8594	27.0386
	0.9	68.4888	-7.7787	-84.3534	-18.7341	0.8921	28.3388
D <sup>-1</sup>	10 <sup>2</sup>	64.5393	-7.2536	-----	-17.8833	0.8853	
	3x10 <sup>2</sup>	26.9275	-7.2532		-23.6636	0.1735	
	5x10 <sup>2</sup>	12.9549	-7.2581		-28.5713	0.0796	
m	0.5	64.5393	-7.2536	-----	-17.8833	0.8853	
	1.0	64.5476	-7.2532		-17.8799	0.8872	
	1.5	64.5551	-7.2581		-17.8771	0.8863	
R	0.2	64.5393	-7.2536	-----	-17.8833	0.8853	
	0.5	64.5277	-7.3875		-17.8780	0.8743	
	0.7	64.4565	-7.6106		-17.8709	0.8868	
Q	5	64.5393	-7.2536	-81.5514	-17.8833	0.8853	25.7847
	10	64.5419		-99.6399	-17.8117	0.9063	31.5237
	15	64.5534		-114.8867	-17.7507	0.9099	36.3536
F	0.5	64.5393	-7.2536	-81.5514	-17.8833	0.8853	25.7847
	2	64.7509	-7.3679	-81.2197	-18.5312	0.9702	
	5	65.4695	-8.0652	-80.7732	-19.2067	1.0577	
					1.2343		

## 5. CONCLUSIONS

We analyze the effect of Hall currents, thermal radiation on unsteady convective heat transfer flow of a nanofluid past a vertical plate in the presence of heat generating sources. Analytical closed form solutions are obtained for both the momentum and the energy equations using the regular perturbation method. Graphical results for various parametric values were presented and discussed for different values. The main findings are summarized as follows:

- The influence of Hall currents the velocity enhances and the thickness of the boundary layer increases in the case of CuO<sub>2</sub> nanofluid, but opposite phenomenon observed in the case of Al<sub>2</sub>O<sub>3</sub> nanofluid case.
- Increase in the rotation parameter R, velocity enhances in the both types of nanofluids.
- With the increase in radiation parameter F, both velocity and temperature enhances in both types of

nanofluids.

- The heat source parameter  $Q$  increases the velocity and temperature decreases in the case of both types of nanofluids.
- The influence of nanoparticle volume fraction parameter  $\phi$  increases the nanofluid primary velocity experiences an enhancement and reduces the nanofluid secondary velocity in the boundary layer.
- With increase of nanoparticle volume fraction parameter increases the thermal conductivity, temperature and thickness of thermal boundary layer enhances.

## 6. REFERENCES

- Agarwal. S. Bhadauri, B.S. Siddheshwar, P.G (2011): Thermal instability of a nanofluid saturating a rotating anisotropic porous medium, STRPM, vol.2, pp:53–64
- Akbarinia, A, Abdolzadeh, Laur. R (2011): Critical investigation of heat transfer enhancement using nanofluids in microchannels with slip and non-slip flow regimes,” Appl Therm Eng, vol.31, pp:556–565.
- Alsaedi. M, .Awais. T Hayat. (2012) Effect of heat generation/absorption on stagnation point flow of nanofluid over a surface with convective boundary conditions,” Comm. Nonlinear Sci. Number Simulation, vol.17, pp:4210–4223.
- Aziz. M. A. E (2010):Flow and heat transfer over an unsteady stretching surface with Hall effects, Meccanica, V.45, pp.97-109.
- Buongiorno. J (2006): Convective transport in nanofluids,” ASME J Heat Tran vol.128, pp:240–250, Ghadimi. A, Saidur. R, Metselaar. H. S. C (2011): A review of nanofluid stability properties and characterization in stationary conditions, Int. J Heat Mass Tran. vol.54(17-18), pp:4051–4068.
- Hajipour. M, A.M.Dekhordi. A. M (2012): Analysis of nanofluid heat transfer in parallel-plate vertical channels partially filled with porous medium, Int. J Therm. Sci., vol. 55, pp:103–113.
- Hamad M. A. A, Ferdows. M (2012): Similarity solutions to viscous flow and heat transfer of nanofluid over nonlinearly stretching sheet, Appl Math Mech Eng Ed, vol.33(7), pp:923–930.
- Hamad M.A.A, Pop. I (2011) Unsteady MHD free convection flow past a vertical permeable flat plate in a rotating frame of reference with constant heat source in a nanofluid, Heat Mass Tran. vol.47, pp:1517–1524
- Hamad. M.A.A (2011): Analytical solution of a natural convection flow of a nanofluid over a linearly stretching sheet in the presence of magnetic field, Int. Comm. Heat Mass Tran, vol.38, pp:487– 492.
- Hickman. K.C.D (1957): Centrifugal boiler compression still”, Ind Eng Chem, vol.49, pp:786–800.
- Hide. R, Robert. P. H (1960): Hydromagnetic flow due to an oscillating plate”, Rev Mod Phys vol.32, pp:799–806.
- Kameswaran. P. K, Narayana. M, Sibanda. P, PVSN Murthy (2012): Hydromagnetic nanofluid flow due to a stretching or shrinking sheet with viscous dissipation and chemical reaction effects, Int. J Heat Mass Tran. vol.55 pp:7587–7595.
- Kesavaiah. D.Ch, Satya.Narayana. P.V, Venkataramana. S (2011) : Effects of the chemical reaction and radiation absorption on an unsteady MHD convective heat and mass transfer flow past a semi-infinite vertical permeable moving plate embedded in a porous medium with heat source and suction, Int. J Appl. Math Mech. vol.7(1), pp:52–69,.
- Kiblinki. P, Phillpot. S. R and Choi. S. U. S (2002): J.A.Eastman,”Mechanism of heat flow in suspensions of nanosized particles (nanofluids), Int. J Heat Mass Tran, vol.42, pp:855–863.
- .Mahbul. I. M, Saidur. R and .Amalina. M. A (2012): Latest developments on the viscosity of nanofluids, Int. J Heat Mass Tran, vol.55(4), pp:874–885.
- .Mazumder. B. S (1991): An exact solution of oscillatory Couette flow in a rotating system” ASME J Appl Mech, vol.58(4), pp:1104–1107.
- Nguyen. C. T, Roy. G, Gauthier. C and Galanis. N (2007) Heat transfer enhancement using  $Al_2O_3$ - water nanofluid for an electronic liquid cooling system, Appl. Thermo Eng, vol.27, pp:1501–1506.
- Norifiah. B. Anuar and Ioan. P. I, Boundary layer flow over a moving surface in a nanofluid with suction or injection”, Acta Mech Sin, vol.28(1), pp:34–40 .
- Rana. P and Bhargava R Flow and heat transfer of a nanofluid over a nonlinearly stretching sheet”, Comm. Nonlinear Sci. Number Simulation, vol. 7, pp:212–226.
- Rushi Kumar. B and Sivaraj. R (2013): Heat and mass transfer in MHD visco-elastic fluid flow over a vertical cone and flat plate with variable viscosity, Int. J Heat Mass Tran, vol.56(1–2), pp:370– 379.
- Salem. A. M, and Aziz. A.M.E (2008): Effect of Hall currents and chemical reaction on hydromagnetic flow of a stretching surface with internal heat generation/absorption, Applied Mathematical Modelling, V.32, pp.1236-1254
- Sarojamma. G, Mahaboobjan. S and Nagendramma. V (2015): Influence of Hall currents on cross diffusive convection in a Mhd boundary layer flow on stretching sheet in porous medium with Heat generation, Int. Jour. Math. Archive, V.6(3), pp.227248.

- Sarojamma. G., Mahaboobjan. S and .Sreelakshmi. K (2015): Effect of Hall current on the flow induced by a stretching surface, *Int. Jour. Sci., and Innovative Math.Res*,V.3(3)pp.1139-1148.
- Satyanarayana. P. V, Venkateswarlu. B. and Venkataramana. S (2013): Thermal radiation and heat source effects on a MHD Nanofluid past a vertical plate in a rotating system with porous medium, *Heat transfer-Asian Research (J.Wiley)*, DOI:10.1002/htj.211001.
- Satyanarayana. P. V, Venkateswarlu. B and Venkataramana. S (2013): Effects of Hall current and radiation absorption on MHD micropolar fluid in a rotating system, *Ain-Shams Eng J*  
<http://dx.doi.org/10.1016/j.asej.2013.02.002>.
- Srinivas. S, A.Subramanyam Reddy. A and Ramamohan. T. R (2012): A study on thermal-diffusion and diffusion-thermo effects in a two-dimensional viscous flow between slowly expanding or contracting walls with weak permeability, *Int. J Heat Mass Tran.* vol.55, pp:3008–3020.
- Tiwari. R. K and Das. M. K(2007): Heat transfer augmentation in a two-sided lid-driven differentially heated square cavity utilizing nanofluids”, *Int. J Heat Mass Tran*, vol.50:2002–2018.
- Oztop. H. F and Abu-Nada. E (2008): Numerical study of natural convection in partially heated rectangular enclosures filled with nanofluids.,*Int.J.Heat and Fluid Flow.*,V.29,pp.1326-1336.